Journal of Radiation Industry 15 (4) : 223 ~ 233 (2021) https://doi.org/10.23042/radin.2021.15.4.223

Microarray Analysis of *Deinococcus radiodurans bphP bphR* Double Mutant

Sangyong Lim[1,2,*], Jong-Hyun Jung[1,2] and Seonghun Im[1]

[1]*Radiation Research Division, Korea Atomic Energy Research Institute, Jeongeup 56212, Republic of Korea*
[2]*Department of Radiation Science and Technology, University of Science and Technology, Daejeon 34113, Republic of Korea*

Abstract - Phytochromes, a family of light-sensing proteins, are widespread in a broad range of organisms, including plants, algae, cyanobacteria, and even non-photosynthetic bacteria. *Deinococcus radiodurans*, which is well known for its extraordinary resistance to γ-radiation, contains bacterial phytochrome photoreceptor (BphP). *D. radiodurans* BphP (DrBphP) is known to dephosphorylate its cognate response regulator DrBphR in response to light and to contribute to mitomycin C (MMC) resistance. In this study, we investigated transcriptional changes in *D. radiodurans bphP bphR* double mutant strain (Δ*bphPR*) to identify genes affected by the DrBphP/R system. Microarray analysis showed that the expression of *dr_0802*, which encodes a putative anti-sigma factor, and *dr_1168*, which encodes a Nudix hydrolase, increased in Δ*bphPR*. Since a gene encoding the alternative sigma factor Sig2 immediately precedes *dr_0802*, the predicted DR_0802 product was named Asf2 (anti-sigma factor 2) here. We constructed *sig2* and *asf2* mutant strains and examined their survival using plates supplemented with MMC under light conditions. A lack of either Sig2 or Asf2 did not cause a change in resistance to MMC compared to the wild type (WT), i.e., there was no difference in survival between WT and mutants. These results suggest that Sig2 and Asf2 are not involved in the DrBphP/R signaling pathway related to MMC resistance.

Key words : Radiation-resistant bacteria, *Deinococcus radiodurans*, Microarray analysis, Bacteriophytochrome, Anti-sigma factor

INTRODUCTION

Deinococcus radiodurans is known for its remarkable resistance to a range of damage caused by various DNA-damaging agents, such as gamma radiation (γ-radiation), UV radiation, desiccation, electrophilic mutagens, and oxidizing agents (Makarova *et al*. 2001). There have been a series of studies dedicated to understanding the molecular mechanisms underlying the development of the extreme resistance phenotype of *D. radiodurans* (Makarova *et al*. 2001; Ghosal *et al*. 2005; Slade and Radman 2011; Timmins and Moe 2016; Lim *et al*. 2019).

Phylogenetic analyses of ribosomal RNAs and several conserved proteins have suggested that *D. radiodurans* is most closely related to *Thermus thermophilus* and that these two genera belong to a distinct branch of eubacteria called the *Deinococcus-Thermus* group (White *et al*. 1999; Omelchenko *et al*. 2005). Given the different phenotypes of *D. radiodurans*, which is a mesophile resistant to γ-radiation, and *T. thermophilus*, which is a thermophile sensitive to γ-radiation, genes associated with their extreme phenotypes were likely acquired, through horizontal gene transfer (HGT), after they diverged from a common ancestor (Om-

* Corresponding author: Sangyong Lim, Tel. +82-63-570-3141, Fax. +82-63-570-3149, E-mail. saylim@kaeri.re.kr

elchenko *et al*. 2005). Studies estimate that between 10% and 15% of the *D. radiodurans* genome has been acquired through HGT (Slade and Radman 2011). Late embryogenesis abundant (LEA) proteins, originally described in plants, are induced under various stress conditions, including desiccation (Makarova *et al*. 2001). Several putative LEA proteins have been identified in *D. radiodurans*, and their inactivation results in increased sensitivity to oxidative stress (Jiang *et al*. 2017; Dai *et al*. 2020). This supports the hypothesis that some of the genes acquired by HGT may directly influence some of the more extraordinary resistance phenotypes associated with *D. radiodurans* when exposed to environmental stresses. One of these genes encodes a phytochrome-like protein (Omelchenko *et al*. 2005).

Phytochromes are a class of photoreceptor that regulates a wide array of light-dependent processes in plants and microorganisms (Burgie and Vierstra 2014). Bacteriophytochromes (BphPs) are a subfamily of the diverse light-responsive phytochrome photoreceptors, which have been identified in cyanobacteria, proteobacteria (both photosynthetic and non-photosynthetic), and actinobacteria, amongst others (Nagano 2016; Gourinchas *et al*. 2019). The gene encoding *D. radiodurans* BphP (DrBphP) is likely derived from a photosynthetic cyanobacterium by HGT because *D. radiodurans* was found to be phylogenetically related to cyanobacteria (Davis *et al*. 1999; Battistuzzi *et al*. 2004). BphPs are typically composed of an N-terminal domain that covalently binds a bilin chromophore and a C-terminal region that transmits the light signal, often through a histidine kinase relay (Wagner *et al*. 2005). The cyanobacterial phytochrome Cph1 from *Synechocystis* shows the same domain organization as DrBphP but differs from DrBphP in its use of phycocyanobilin in place of biliverdin, as the chromophore (Nagano 2016). The inactivation of *cph1* decreases cell growth under continuous far-red light and alters the red light-dependent expression of genes involved in transcription, translation, and chlorophyll biosynthesis (Fledler *et al*. 2004; Hübschmann *et al*. 2005). The reduction of cell growth is also observed in *D. radiodurans bphP* mutant compared with wild type when grown under intense light (Davis *et al*. 1999), but transcriptional changes associated with *bphP* mutation have not been studied.

Bacteria adapt to environmental changes using two-component signaling systems (TCSs). A sensor protein histidine kinase (HK) catalyzes its autophosphorylation and transfers the phosphoryl group to a response regulator (RR), which then regulates gene expression and facilitates specific survival responses to various environmental changes (Laub and Goulian 2007). HKs can also act as phosphatases that remove the phosphate group from the phosphorylated RR to reset TCS (Goulian 2010). DrBphP contains an HK domain, and its putative cognate RR, DrBphR, is encoded downstream in the *D. radiodurans bph* operon (Bhoo *et al*. 2001). However, DrBphP is known to function as a light-activated phosphatase that can dephosphorylate DrBphR, unlike other typical BphPs exhibiting kinase activities (Multamäki *et al*. 2021).

In this study, we investigated changes in gene expression from a *bphP bphR* double mutant strain to identify downstream signaling pathways coupled to DrBphP/R in *D. raidiodurans*.

MATERIALS AND METHODS

1. Bacterial strains and growth conditions

A wild-type *D. radiodurans* strain (ATCC 13939) and its isogenic *bphP bphR* double mutant strain (Jung *et al*. 2021) were used in this study. The cells were grown at 30°C in TGY (0.5% tryptone, 0.3% yeast extract, and 0.1% glucose) broth under white light (~150 $\mu mol \cdot m^{-2}s^{-1}$). A seed culture that had been grown overnight was inoculated into fresh TGY broth at a 1 : 100 dilution. For mitomycin C (MMC) treatment, 5 $\mu g \cdot mL^{-1}$ of MMC was added into a culture grown to the early log phase ($OD_{600} \approx 1.0$), and the culture was incubated for 1 hr. Kanamycin (8 $\mu g \cdot mL^{-1}$) was used when necessary.

2. Oligonucleotide microarrays

The microarray was constructed by MYcroarray, Inc. (Ann Arbor, MI, USA) using the genome information for sequenced *D. radiodurans* R1 (White *et al*. 1999). A total of 3,082 gene-specific probes (45 nucleotides in length) were designed, which cover ~99.4% of the 3,102 protein-coding genes on the R1 chromosome. The microarray used in this study consists of 16,320 features. Of these, 12,328 spots were used to represent the 3,082 genes (four replicates of a probe), and the remaining 3,992 features were used for internal quality control. Three arrays per slide were generated by *in situ* syntheses using a proprietary light-directed oligonucleotide synthesis technology (www.mycroarray.com).

3. Probe preparation and hybridization

The total bacterial RNA was isolated using RiboEX reagent (GeneAll, Korea), treated with DNase, and purified using RNeasy® Mini kit (Qiagen, Germany) according to the manufacturer's instructions. The quality and integrity of the prepared total RNAs were confirmed with the use of an Agilent 2100 bioanalyzer (Agilent Technologies, Inc., Palo Alto, CA, USA) and Gene Quant pro (Amersham Pharmacia Biotech, UK). The extracted RNA was amplified and labeled using Agilent's Low Input Quick Amp WT Labeling Kit (Agilent Technologies, Inc.) according to the manufacturer's instructions. Briefly, 100 ng of total RNA was mixed with WT Primer Master Mix and incubated at 65°C for 10 min. Following the addition of the cDNA Master Mix, the reaction mixture was incubated at 40°C for 2 hr for reverse transcription and at 70°C for 10 min to stop the reaction. Transcription Master Mix was added to the reaction mixture, and the mixture was incubated at 40°C for 2 hr to generate the labeled cRNA probes. The amplified and labeled cRNA was purified on RNase mini column (Qiagen) according to the manufacturer's protocol and quantified using an ND-1000 spectrophotometer (NanoDrop Technologies, Inc., Wilmington, DE, USA). After the fragmentation of Cy3-(the control sample) and Cy5-labeled cRNA (the experimental sample), they were hybridized to the arrays. The hybridizations were conducted at 57°C for 17 hours in an Agilent Hybridization oven and washed following the manufacturer's protocol (Agilent Technologies, Inc.).

4. Data acquisition and analysis

The scans were performed with an Agilent DNA microarray scanner (Agilent Technologies, Inc.) using Agilent Feature Extraction software 10.7 (Agilent Technologies, Inc.). The signal intensities were quantified using GeneSpringGX 7.3.1 software (Agilent Technologies, Inc.). The genes were filtered by removing the flag-out genes in each experiment. The normalization of gene expression by a LOWESS regression was applied for 3 data obtained from 3 biological replicates. The genes were considered to be differentially expressed when the logarithmic gene expression ratios had more than a 2-fold difference in the expression level. The statistical significance of the data was determined by Student's t-test. *P*-values of less than 0.05 were taken to be statistically significant.

5. Quantitative real-time PCR (qRT-PCR)

A 10 mL culture was grown to the early log phase ($OD_{600} \approx 1.0$) under white light. After centrifugation, the cell pellets were re-suspended in 2 mL of RiboEX reagent (GeneAll Biotechnology, Korea) and lysed in a Precellys 24 bead beater (Bertin Technologies, France) using 0.1 mm diameter Zirconia/Silica beads (Biospec Products, USA). The total RNA was purified using the RNeasy® Mini kit (Qiagen, Germany) and RNase-free DNase (Qiagen) according to the manufacturer's instructions. For real-time PCR analysis, cDNA was synthesized from 1 μg of total RNA using the Primescript 1st strand cDNA Synthesis Kit (Takara Bio Inc., Japan) as recommended in the manufacturer's instructions. Real-time qPCR amplification was performed with SYBR Premix Ex Taq (Takara) on an Eco™ Real-Time PCR System (Illumina, USA). PCR reactions were performed as follows one cycle of 95°C for 5 min and then 40 cycles of 95°C for 10 s and 60°C for 30 s. The housekeeping gene *dr1343*, which encodes glyceraldehyde-3-phosphate dehydrogenase with an expression level that is unaffected by ionizing radiation (Earl *et al*. 2002), was used as an internal control. Forward and reverse primers used in qRT-PCR are listed in Table 1.

6. Construction of mutant strains

D. radiodurans sig2 (*dr_0804*) and *asf2* (*dr_0802*) mutant strains were constructed using the deletion mutagenesis technique, as previously described (Im *et al*. 2013). The primers for each target gene were designed with appropriate restriction enzyme sequences (Table 1). Briefly, the upstream and downstream regions were amplified using the primer pairs corresponding to the target genes. After PCR amplification, the upstream and downstream fragments were digested with *Xho*I/*EcoR*V and *Xba*I/*Pst*I, respectively, and then cloned into the corresponding sites of pKatAPH3. The resulting plasmids were transformed into *D. radiodurans*, and the transformants were screened on TGY agar plates supplemented with kanamycin. The disruption of the target genes was confirmed by diagnostic PCR.

7. Survival assay

The cells grown to log phase ($OD_{600} \approx 1.0$) were serially diluted 10-fold in a fresh TGY medium. Then 10-μL of each dilution was spotted on TGY plates supplemented with

Table 1. Primers used in this study

Mutant construction		RE*
Asf2-Up-F	5′-attctcgagaaaccgctcaccggatggac-3′	*Xho*I
Asf2-Up-R	5′-tatgatatcctgttcgccagcgacgtga-3′	*EcoR*V
Asf2-Dw-F	5′-aaggatccgtgcaaagcccagaaccagc-3′	*BamH*I
Asf2-Dw-R	5′-tatctgcagcaaggagtcgaggacgc-3′	*Pst*I
Sig2-Up-F	5′-attctcgagcacggcttgcagtgg-3′	*Xho*I
Sig2-Up-R	5′-gtatgatatcgaacagcgcgagccggagac-3′	*EcoR*V
Sig2-Dw-F	5′-aaggatccgtcgcgcagcacctgttcg-3′	*BamH*I
Sig2-Dw-R	5′-tatctgcagggtcacgagctgcaccttgc-3′	*Pst*I
qRT-PCR	Forward	Reverse
DR_0592	5′-cgaggactggcaggagtt-3′	5′-cggtcaaattcttcctccat-3′
DR_0892	5′-ccagctggaggctgtgta-3′	5′-agccgccacaactggtag-3′
DR_1168	5′-tgcaactggtggactttc-3′	5′-gcgactctgggatagaccct-3′
DR_1342	5′-gtgaacgacgagcagtacga-3′	5′-gtggtcatgatggccttctc-3′

* Restriction enzyme (RE) recognition sites are underlined in the sequences.

various concentrations of MMC. The plates were incubated in the dark or under red light (700 nm) for 2 days (LED light incubator DS210-156 SF, Daewon Science, Korea) before the enumeration of colonies.

RESULTS

1. Characterization of genes affected by *bphP bphR* mutation

We determined the genes whose expression was altered by the absence of *bphP* and *bphR* using DNA microarray. The wild-type (WT) and *bphP bphR* double mutant (Δ*bphPR*) strains grown to the early log phase ($OD_{600} \approx 1.0$) under light were harvested for RNA extraction, and then the extracted total RNAs were subjected to microarray analysis. We screened the genes showing a statistically significant expression ratio (p-value < 0.05) of at least a 2-fold change relative to the wild type. Only five and three genes were induced and reduced, respectively, in the *bphPR* mutants, compared to WT (Table 2). We found that DrBphP contributed to the *D. radiodurans* resistance against the DNA alkylating agent mitomycin C (MMC) in red and far-red light (Jung *et al*. 2021). Thus, we incubated the log-phase cells for 1 hr in the presence of MMC (5 $\mu g \cdot mL^{-1}$), in which the phenotype of Δ*bphPR* was manifested (Jung *et al*. 2021). However, the number of genes affected by *bphP bphR* mutation was not significantly changed: six genes were induced and five genes were reduced in the *bphPR* mutants when the cells were exposed to MMC (Table 2).

The down-regulated gene, *dr_0592*, and the up-regulated genes, *dr_0802* and *dr_1168*, were found in both experimental conditions, suggesting that these three genes are affected by the *bphP bphR* double mutation whether DNA damage occurs or not. The expression of these genes was validated by quantitative real-time PCR (qRT-PCR) (Fig. 1). Expansion of the Nudix hydrolase family is one of the most prominent features of the *D. radiodurans* genome, in which 23 Nudix hydrolases are encoded (Makarova *et al*. 2001). The MutT protein, the prototype of this family, is a pyrophosphohydrolase, and the Nudix hydrolases are hypothesized to function as house-cleaning enzymes that potentially destroy deleterious damaging products (Makarova *et al*. 2001). DR_1168 is one of the Nudix hydrolases and contains a Zn-ribbon module, which is probably involved in nucleic acid binding (Makarova *et al*. 2001). Further research is warranted to investigate DR_1168 is functionally associated with DrBphP.

2. Reannotation of the *asf2* open reading frame (ORF)

Among the up-regulated genes in Δ*bphPR*, *dr_0802* encodes a putative anti-sigma factor, named Asf2 here (anti-sigma factor of Sig2) (Table 2). Because there was an additional ORF *dr_0803* between *sig2* and *asf2* (Fig. 2A), we performed sequence analysis using the Basic Local Alignment Search Tool (BLAST) to know if the gene

Table 2. Genes with altered expression in Δ*bphPR* mutants

–			MMC treatment		
Gene ID	Description	Ratio[a]	Gene ID	Description	Ratio[a]
	Up-regulated			**Up-regulated**	
DR_0070	Hypothetical protein	2.068	DR_0033	Enamine deaminase RidA	2.128
DR_0594	Glycogen synthase	2.003	DR_0778	3-dehydroquinate dehydratase	2.031
DR_0802	Anti-sigma factor	2.103	DR_0802	Anti-sigma factor	2.289
DR_1168	MutT/Nudix family protein	2.066	DR_1168	MutT/Nudix family protein	2.121
DR_2378	Hypothetical protein	2.203	DR_1412	Conserved hypothetical protein	2.049
			DR_2469	ABC transporter, ATP-binding protein	2.013
	Down-regulated			**Down-regulated**	
DR_0592	Hypothetical protein	0.468	DR_0592	Hypothetical protein	0.488
DR_0913	Hypothetical protein	0.497	DR_0674	Arginosuccinate synthase	0.382
DR_1082	Light-repressed protein A	0.411	DR_0675	Acetyltransferase (GNAT) family	0.344
			DR_0683	Conserved hypothetical protein	0.441
			DR_1849	Peptide methionine sulfoxide reductase	0.412

[a]The ratio is the fold increase in mRNA level in Δ*bphPR* mutants compared to wild type.

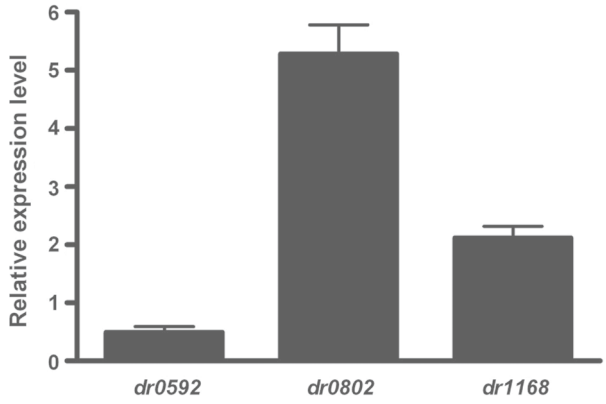

Fig. 1. Validation of microarray data using qRT-PCR. The mRNA levels of *dr_0592*, *dr_0802*, and *dr_1168* were determined using real-time PCR. Cultures were grown under white light, and MMC (5 μg · mL^{-1}) was added into the cultures at an OD_{600} nm of 1.0. Total RNA was isolated from the MMC-treated cultures after 1 h of incubation. The relative expression values were determined by dividing the mRNA levels from wild-type by the mRNA levels from *bphPR* mutant strains. The expression levels of the target genes were normalized to the *dr_1343* gene. The means ± standard deviations of three independent experiments performed in duplicate are shown.

arrangement of *sig2* (*dr_0804*)-*dr_0803*-*asf2* (*dr_0802*) is conserved in other *D. radiodurans* strains. We retrieved the available genome sequences of *D. radiodurans* strains, such as ATCC 13939, DSM 20539, BNK-50, and BND-54, from the NCBI nucleotide database (http://www.ncbi.nlm.nih.gov/nucleotide/) and analyzed the predicted ORFs coding for Asf2. We found that the ORFs encode the identical Asf2 protein (WP_027479976.1) with a length of 246 amino acids (aa), which is longer than the predicted Asf2 protein consisting of 132 aa (AAF10381.1) encoded by *dr_0802* (Fig. 3).

The genome of the type strain *D. radiodurans* R1 ATCC BAA816 was sequenced by White *et al*. and released in 1999 (White *et al*. 1999) and resequenced by Hua and Hua in 2016 (Hua and Hua 2016). BLASTN analysis revealed that the *asf2* sequence (741 base pairs long) in strain R1-2016, which was used for resequencing in 2016, is completely aligned to the nucleotide sequence of the region encompassing *dr_0803* and *dr_0802* in the previously sequenced strain R1, R1-1999 (Figs. 2A and 4). The R1-2016 *asf2* gene has additional cytosines at positions 193 and 426, respectively, which are not present in the sequence of strain R1-1999, and these two changes make it possible to encode the full-length Asf2 protein (Fig. 4). Accordingly, in *D. radiodurans*, Sig2 is encoded by the *dr_0804* gene, and its immediate downstream gene *dr_0802m* encodes the anti-sigma factor Asf2 (Fig. 2B).

3. Effects of *sig2* and *asf2* mutation on the light-dependent MMC resistance of *D. radiodurans*

Anti-sigma factors modulate numerous genes controlled by alternative sigma factors by protein interaction with a target sigma factor (Helmann 1999). Hence, it is likely that DrBphP/R can affect the light-dependent MMC resistance

via Sig2 by modulating the *asf2* gene expression. We constructed *D. radiodurans sig2* (Δ*sig2*) and *asf2* (Δ*asf2*) mutant strains and investigated the MMC resistance of the mutants under our experimental conditions (see 7. Survival assay). The mutant strains exhibited a similar survival pattern to the WT, including a further reduction in survival when grown in the dark. MMC challenge with 300 nM MMC resulted in a 2.7∼2.9-log reduction in the survival rates of the all strains tested, and cells grown in the dark showed an approximately 1-log reduction in survival relative to the illuminated cells (Fig. 5). These imply that Sig2 and Asf2 are not mediators between DrBphP/R and MMC resistance in illuminated cells. This area warrants further investigation to identify the genes and/or proteins regulated by DrBphP/R.

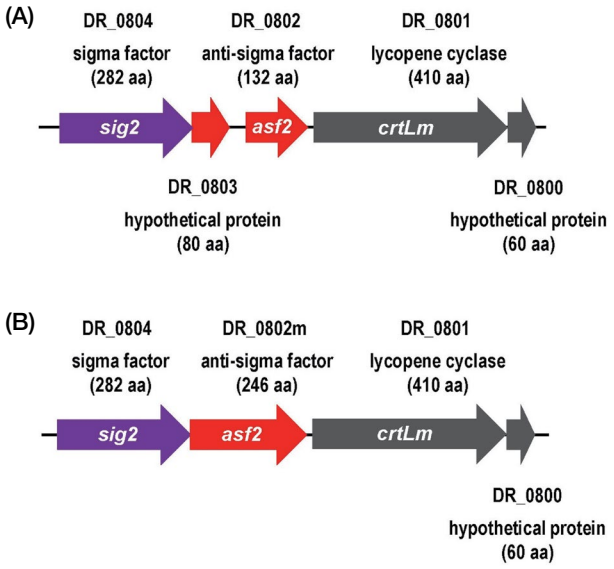

Fig. 2. Gene arrangement of the *dr_0800-dr_0804* gene cluster in *D. radiodurans* strain R1-1999 (A) and strain R1-2016 (B). Each protein is shown with its corresponding locus tag.

4. A literature review of BphPs sharing the same domain architecture with DrBphP: focusing on downstream regulators

Since their discovery in plants, phytochromes have also been identified in cyanobacteria, proteobacteria (both photosynthetic and non-photosynthetic), and actinobacteria, amongst others (Burgie and Vierstra 2014; Nagano 2016). These BphPs are typically composed of an N-terminal photosensory module (PSM) including a PAS (Period/Arnt/Single-Minded) domain, a signature GAF (cGMP phosphodiesterase/adenylyl cyclase/FhlA) domain, and a PHY (phytochrome-specific) domain, and a C-terminal output module (OPM) including HK (Burgie and Vierstra 2014). However, some lack the upstream PAS domain or exhibit some deviation from the typical PAS-GAF-PHY tridomain architectures associated with these proteins. OPMs harboring diguanylate cyclase, phosphodiesterase, and HK-RR fusion (hybrid two-component HK) domains have also been found in BphPs (Auldridge and Forest 2011; Burgie and Vierstra 2014). DrBphP has a common architecture consisting of an N-terminal PSM with three conserved domains (PAS-GAF-PHY) and a C-terminal HK module.

The photosynthetic bacterium *Rhodopseudomonas palustris* contains six putative bacteriophytochrome-related proteins (RpBphPs) (Vuillet *et al*. 2007). Among them, RpBphP2 and RpBphP3 are composed of the PAS-GAF-PHY tridomain and a C-terminal HK domain described for DrBphP (Auldridge and Forest 2011). The two genes encoding RpBphP2 and RpBphP3 and three genes encoding RRs constitute an operon (Giraud *et al*. 2005). RpBphP2 and RpBphP3 act in tandem with the three RRs to sense light quality and upregulate the synthesis of the photosynthetic apparatus, light-harvesting complex 4 (Fixen *et al*. 2019). Many phytochromes have been characterized in the order

```
AAF10381.1          ------------------------------------------------------------------------------
WP_027479976.1        1 MSVTRQELLALALGQLSSEDQQRVGQALDHDPALRTALRRDLDALTSLLADLDVQAQTVPPGADLRLLERVRAETAKQQP  80

AAF10381.1            1 --------------MGAACAAGARPRAGS--------------------GLCTAPGRRRRLPYAAVPNAQLEAVYGPGGA  46
WP_027479976.1       81 VAPVGRPAAPPALTPAPAAPARTRPAGGRFPGPSWALPALLALGLALVLGFALRPAGDAASRYAAVPNAQLEAVYGPGGA  160

AAF10381.1           47 VARLVRLDDGRVYVRMDRPLEAGRIYQLWRLLPGPANASLPRSLGLFASDVMTHPMPLQAVLAVSVEPPGGSSQPSTPLL  126
WP_027479976.1      161 VARLVRLDDGRVYVRMDRPLEAGRIYQLWRLLPGPANASLPRSLGLFASDVMTHPMPLQAVLAVSVEPPGGSSQPSTPLL  240

AAF10381.1          127 FKFRLR  132
WP_027479976.1      241 FKFRLR  246
```

Fig. 3. Alignment of amino acid sequences of Asf2. Black letters on light gray shading represent 100% identity. Protein sequences obtained from the NCBI database are distinguished by the accession numbers. AAF10381.1; *D. radiodurans* R1-1999 and WP_027479976.1; *D. radiodurans* R1-2016, ATCC 13939, DSM 20539, BNK-50, and BND-54.

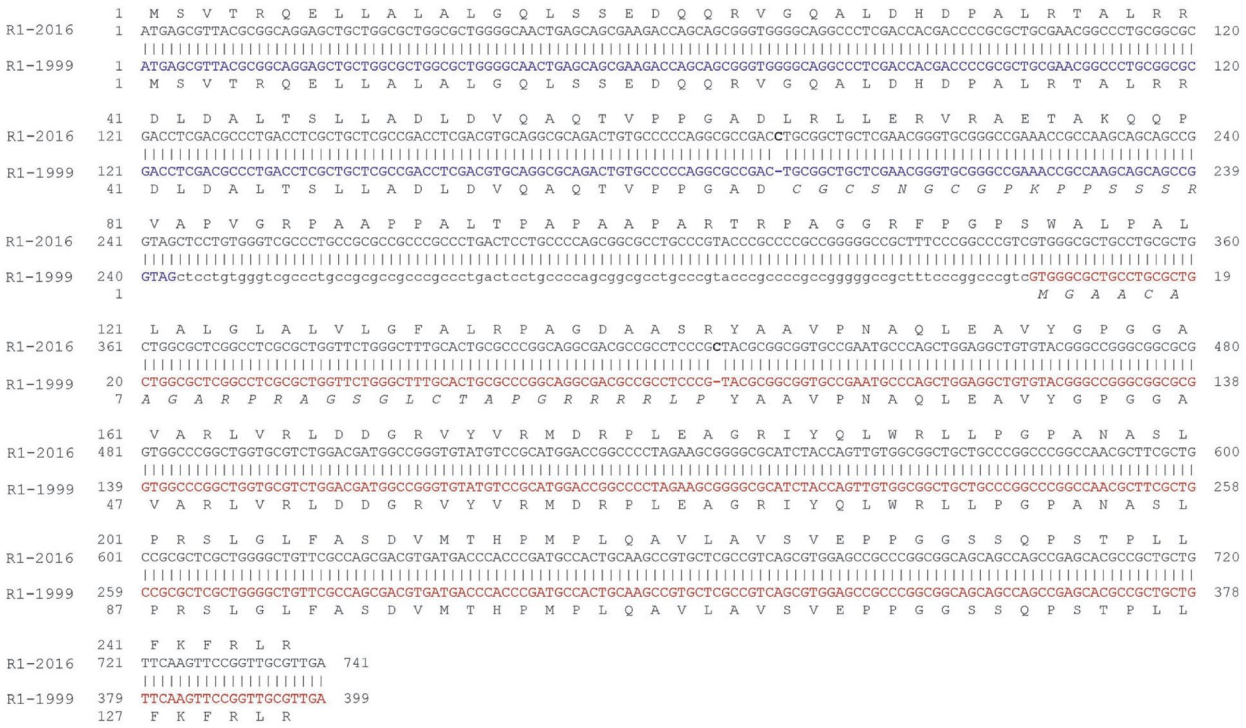

Fig. 4. Nucleotide sequence of the *asf2* gene. The region of chromosome I (R1-2016, NZ_CP015081.1) between coordinates 1,909,645 and 1,910,385 bp was aligned to the region of chromosome I (R1-1999, AE000513.1) between coordinates 815,879 and 816,597. The nucleotide sequences are numbered according to the initiation codon of *dr_0802m* (*asf2*) in R1-2016 and *dr_0803* and *dr_0802* in R1-1999 (refer to Fig. 2). The deduced amino acid sequence is shown above the nucleotide sequence of the R1-2016 *asf2* gene and below the R1-1999 *dr_0803* (blue) and *dr_0802* (red) genes. Predicted noncoding regions in the genome of R1-1999 are shown in lower case. The nucleotides omitted in the sequence of *dr_0803* and *dr_0802* are shown in bold in the sequence of R1-2016 *asf2*. The reading frames affected by the sequencing errors are shown in italics.

Rhizobiales, which fix nitrogen and are symbiotic with plant roots, including photosynthetic *Rhodopseudomonas* and non-photosynthetic *Agrobacterium* species (Rottwinkel *et al*. 2010). *Agrobacterium fabrum* (former: *Agrobacterium tumefaciens*) containing two phytochromes, Agp1 and Agp2. Agp1 is a typical PAS-GAF-PHY-HK, and Agp2 expresses a unique type of a hybrid HK carrying RR at its C-terminus (Karniol and Vierstra 2004; Lamparter *et al*. 2017). In *A. fabrum agp* mutants, light regulation of gene expression, motility, infectivity (T-DNA transfer from bacterium to plants), and conjugation (plasmid DNA transfer among bacteria) have all been evaluated. A clear phytochrome effect was found for the conjugation of *A. fabrum* (Lamparter *et al*. 2017). It has been recently reported that Agp1 and Agp2 interact with each other and affect phosphorylation of the other phytochrome (Xue *et al*. 2019). *Azospirillum brasilense*, a non-photosynthetic rhizobacterium, harbors a pair of BphPs, one of which, AbBphP1, is a homolog of Agp1. The AbBphP1 mutant is sensitive to red light in minimal malate media and photodynamic stress in-

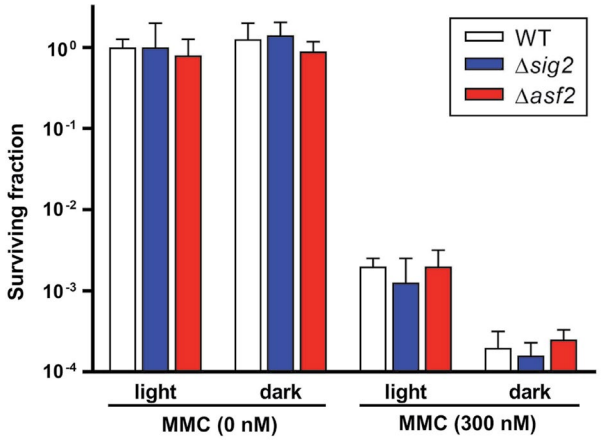

Fig. 5. Survival of *sig2* and *asf2* mutants during continuous exposure to MMC. *D. radiodurans* wild-type (WT) and *sig2* (Δ*sig2*) and *asf2* (Δ*asf2*) mutant strains were grown to log phase, then serially diluted and spotted on TGY plates supplemented with the indicated concentrations of MMC. The plates were incubated under red light (700 nm) or no light (dark) conditions for 2 days before the enumeration of colonies. The surviving fraction was expressed relative to the survival of WT grown under light conditions without MMC (arbitrarily set at 1). The error bars represent the standard deviation of three independent experiments (n = 3).

troduced by toluidine blue (TB) (Kumar *et al*. 2012). In *A. brasilense*, a gene encoding AbBphP1 is the first gene of a tricistronic operon followed by genes encoding an RR and HK, respectively (Kumar *et al*. 2012). Thus, it is likely that all the three proteins form a regulatory cascade in response to light, but its mechanism has not yet been revealed.

The non-photosynthetic plant pathogen *Pseudomonas syringae* has two BphPs, PsBphP1 and PsBphP2. PsBphP1 with the prototypical domain arrangement of BphPs negatively regulates swarming motility in response to red and far-red light and affects virulence and plant colonization (Bhoo *et al*. 2001; Wu *et al*. 2013; McGrane and Beattie 2017). PsBphP1 lacks a clear candidate RR, hence its' signaling involves a bacteriophytochrome-regulated swarming inhibitor (Bsi) and an acyl-homoserine lactone (AHL) instead of RR (McGrane and Beattie 2017). The non-photosynthetic bacterium *Ramlibacter tataouinensis* isolated from the desert presents with a unique light-controlled cell cycle, which alternates between cysts in the dark and motile rods in red light. The two *R. tataouinensis* BphPs, RtBphP1 and RtBphP2, which both display the classical BphP architecture, are involved in the rapid rod division phase of the cell cycle (Baker *et al*. 2016; De Luca *et al*. 2019). In the dark, the rod division is repressed by the phosphorylation of the cognate RR RtBRR, which is occurred through indirect cooperation between RtBphP1 and RtBphP2 (De Luca *et al*. 2019). Taken together, it can be assumed that downstream regulators link BphPs to critical functions of cells because the physiological roles of BphPs are varied depending on host cells although they have the same domain architecture, PAS-GAF-PHY-HK.

DISCUSSION

In this study, we could find only 16 genes affected by *bphP bphR* mutation (Table 2). The small number of genes affected by BphP has been reported in *A. fabrum*. Only eight out of 4500 genes showed differential expression between light and dark, and the difference disappeared in an *agp1 agp2* double mutant (Lamparter *et al*. 2017). But on the other hand, a marginal effect of *bphP bphR* mutation on gene expression can be attributable to the experimental condition used in this study. The previous studies used a plate assay, in which cells were spotted on plates and incubated under illumination (Davis *et al*. 1999; Jung *et al*. 2021). However, because cells were grown in liquid media for RNA extraction in this study, it is unlikely that light is transmitted evenly across the media. In addition, the photosynthetic photon flux density (PPFD) value of light (~150 $\mu mol \cdot m^{-2}s^{-1}$) used in this study was lower than that of light (~350 $\mu mol \cdot m^{-2}s^{-1}$) used in the previous study (Davis *et al*. 1999). Hence, the marginal effect observed in Δ*bphPR* may be explained as a result of the limited penetration of light.

Among the up-regulated genes in Δ*bphPR*, we focused on the anti-sigma factor DR_0802 because the gene expression of *Pseudomonas aeruginosa* BphP is associated with the alternative sigma factor, RpoS (Barkovits *et al*. 2011). *D. radiodurans* has three sigma factors, including one that is the primary sigma factor σ^{70} (RpoD, DR_0916), and the others belong to a specific group of alternative sigma factors, the so-called extracytoplasmic function sigma factors (σ^{ECF}), designated Sig1 (DR_0180) and Sig2 (DR_0804) (Schmid and Lidstrom 2002; Souza *et al*. 2014). In general, an σ^{ECF} is co-transcribed with its cognate anti-sigma factor, which serves as a negative regulator by preventing the interaction between σ^{ECF} and RNA polymerase until an encounter with specific environmental cues that necessitate σ^{ECF} (Veyrier *et al*. 2020). Here, we found that the initial annotation of the *dr_0804* (*sig2*)-*dr_0803*-*dr*_0802 (*asf2*) operon was wrong due to some mistakes in the R1-1999 sequence (Fig. 4). The DR_0804 Sig2 is co-transcribed with the DR_0802m Asf2 like other σ^{ECF} (Fig. 2).

The relationship of either Sig2 or Asf2 with DrBphP was examined by survival assay of *sig2* and *asf2* mutant strains under continuous exposure to MMC. Most studies use a two-step method consisting of MMC exposure in liquid media and subsequent cell plating, named an acute exposure assay here, to determine the MMC resistance of *D. radiodurans* wild-type and mutant strains (Kitayama *et al*. 1983; Agostini *et al*. 1996; Im *et al*. 2013; Zhang *et al*. 2015; Li *et al*. 2017). However, the deletion of *bphP* did not sensitize *D. radiodurans* to MMC when the cells were incubated following MMC treatment (Jung *et al*. 2021). Hence, we opted to use a plate assay, in which cells were spotted on plates supplemented with MMC and incubated under illumination, named a chronic exposure assay, and found the light-dependent protective role of DrBphP/R (Jung *et al*. 2021). The chronic exposure assay showed that *D. radiodurans* WT grown under light conditions exhibited an increase in survival compared to cells grown in the dark (Fig. 5), which is consistent with the previous result (Jung *et al*. 2021). How-

ever, Sig2 and Asf2 did not contribute to the MMC resistance of *D. radiodurans* under our experimental conditions (Fig. 5)

DrBphP exerts its protective effect through counteracting two RRs, DrBphR and DR_0781, regarding the light-dependent MMC resistance (Jung *et al*. 2021). DR_0781 is a member of OmpR/PhoB family RR containing DNA-binding domain, while DrBphR is a CheY-like single domain RR without any output domains, suggesting that DR_0781 regulates expression of target genes via direct binding on their promoter regions. Further research is needed to identify the genes regulated by DR_0781 to understand the underlying mechanism of DrBphP-mediated effects.

ACKNOWLEDGEMENTS

This research was supported by the Nuclear R&D program of the Ministry of Science and ICT (MSIT), Republic of Korea.

REFERENCES

Agostini HJ, Carroll JD and Minton KW. 1996. Identification and characterization of *uvrA*, a DNA repair gene of *Deinococcus radiodurans*. *J. Bacteriol*. **178**:6759-6765.

Auldridge MC and Forest KT. 2011. Bacterial phytochromes: more than meets the light. *Crit. Rev. Biochem. Mol. Biol*. **46**:67-88.

Baker AW, Satyshur KA, Morales NM and Forest KT. 2016. Arm-in-arm response regulator dimers promote intermolecular signal transduction. *J. Bacteriol*. **198**:1218-1229.

Barkovits K, Schubert B, Heine S, Scheer M and Dinkel NF. 2011. Function of the bacteriophytochrome BphP in the RpoS/Las quorum-sensing network of *Pseudomonas aeruginosa*. *Microbiology* **157**:1651-1664.

Battistuzzi FU, Feijao A and Hedges SB. 2004. A genomic timescale of prokaryote evolution: insights into the origin of methanogenesis, phototrophy, and the colonization of land. *BMC Evol. Biol*. **4**:44.

Bhoo SH, Davis SJ, Walker J, Karniol B and Vierstra RD. 2001. Bacteriophytochromes are photochromic histidine kinases using a biliverdin chromophore. *Nature* **414**:776-779.

Burgie ES and Vierstra RD. 2014. Phytochromes: an atomic perspective on photoactivation and signaling. *Plant Cell* **26**: 4568-4583.

Dai J, Gao K, Yao T, Lu H, Zhou C, Guo M, Dai S, Wang L, Xu H, Tian B, Hua Y and Zhao Y. 2020. Late embryogenesis abundant group3 protein (DrLEA3) is involved in antioxidation in the extremophilic bacterium *Deinococcus radiodurans*. *Microbiol. Res*. **240**:126559.

Davis SJ, Vener AV and Vierstra RD. 1999. Bacteriophytochromes: phytochrome-like photoreceptors from nonphotosynthetic eubacteria. *Science* **286**:2517-2520.

De Luca G, Fochesato S, Lavergne J, Forest KT, Barakat M, Ortet P, Achouak W, Heulin T and Verméglio A. 2019. Light on the cell cycle of the non-photosynthetic bacterium *Ramlibacter tataouinensis*. *Sci. Rep*. **9**:16505.

Earl AM, Mohundro MM, Mian IS and Battista JR. 2002. The IrrE protein of *Deinococcus radiodurans* R1 is a novel regulator of *recA* expression. *J. Bacteriol*. **184**:6216-6224.

Fixen KR, Oda Y and Harwood CS. 2019. Redox regulation of a light-harvesting antenna complex in an anoxygenic phototroph. *mBio* **10**:e02838-19.

Fledler B, Broc D, Schubert H, Rediger A, Börner T and Wilde A. 2004. Involvement of cyanobacterial phytochromes in growth under different light qualities and quantities. *Photochem. Photobiol*. **79**:551-555.

Ghosal D, Omelchenko MV, Gaidamakova EK, Matrosova VY, Vasilenko A, Venkateswaran A, Zhai M, Kostandarithes HM, Brim H, Makarova KS, Wackett LP, Fredrickson JK and Daly MJ. 2005. How radiation kills cells: survival of *Deinococcus radiodurans* and *Shewanella oneidensis* under oxidative stress. *FEMS Microbiol. Rev*. **29**:361-375.

Giraud E, Zappa S, Vuillet L, Adriano JM, Hannibal L, Fardoux J, Berthomieu C, Bouyer P, Pignol D and Verméglio A. 2005. A new type of bacteriophytochrome acts in tandem with a classical bacteriophytochrome to control the antennae synthesis in *Rhodopseudomonas palustris*. *J. Biol. Chem*. **280**:32389-32397.

Gourinchas G, Etzl S and Winkler A. 2019. Bacteriophytochromes - from informative model systems of phytochrome function to powerful tools in cell biology. *Curr. Opin. Struct. Biol*. **57**:72-83.

Goulian M. 2010. Two-component signaling circuit structure and properties. *Curr. Opin. Microbiol*. **13**:184-189.

Helmann JD. 1999. Anti-sigma factors. *Curr. Opin. Microbiol*. **2**:135-141.

Hua X and Hua Y. 2016. Improved complete genome sequence of the extremely radioresistant bacterium *Deinococcus radiodurans* R1 obtained using PacBio single-molecule sequencing. *Genome Announc*. **4**:e00886-16.

Hübschmann T, Yamamoto H, Gieler T, Murata N and Börner T. 2005. Red and far-red light alter the transcript profile in the cyanobacterium *Synechocystis* sp. PCC 6803: impact of cyanobacterial phytochromes. *FEBS Lett*. **579**:1613-1618.

Im S, Song D, Joe M, Kim D, Park DH and Lim S. 2013. Comparative survival analysis of 12 histidine kinase mutants of *Deinococcus radiodurans* after exposure to DNA-damag-

ing agents. *Bioproc. Biosyst. Eng.* **36**:781-789.

Jiang S, Wang J, Liu X, Liu Y, Guo C, Zhang L, Han J, Wu X, Xue D, Gomaa AE, Feng S, Zhang H, Chen Y, Ping S, Chen M, Zhang W, Li L, Zhou Z, Zuo K, Li X, Yang Y and Lin M. 2017. DrwH, a novel WHy domain-containing hydrophobic LEA5C protein from *Deinococcus radiodurans*, protects enzymatic activity under oxidative stress. *Sci. Rep.* **7**:9281.

Jung J-H, Jeong S, Im S, Kim M-K, Seo HS and Lim S. 2021. Lack of the bacterial phytochrome protein decreases *Deinococcus radiodurans* resistance to mitomycin C. *Front. Microbiol.* **12**:659233.

Karniol B and Vierstra RD. 2004. The HWE histidine kinases, a new family of bacterial two-component sensor kinases with potentially diverse roles in environmental signaling. *J. Bacteriol.* **186**: 445-453.

Kitayama S, Asaka S and Totsuka K. 1983. DNA double-strand breakage and removal of cross-links in *Deinococcus radiodurans*. *J. Bacteriol.* **155**:1200-1207.

Kumar S, Kateriya S, Singh VS, Tanwar M, Agarwal S, Singh H, Khurana JP, Amla DV and Tripathi AK. 2012. Bacteriophytochrome controls carotenoid-independent response to photodynamic stress in a non-photosynthetic rhizobacterium, *Azospirillum brasilense* Sp7. *Sci. Rep.* **2**:872.

Lamparter T, Krauß N and Scheerer P. 2017. Phytochromes from *Agrobacterium fabrum*. *Photochem. Photobiol.* **93**: 642-655.

Laub MT and Goulian M. 2007. Specificity in two-component signal transduction pathways. *Annu. Rev. Genet.* **41**:121-145.

Li T, Weng Y, Ma X, Tian B, Dai S, Jin Y, Liu M, Li J, Yu J and Hua Y. 2017. *Deinococcus radiodurans* toxin-antitoxin MazEF-dr mediates cell death in response to DNA damage stress. *Front. Microbiol.* **26**:1427.

Lim S, Jung J-H, Blanchard L and de Groot A. 2019. Conservation and diversity of radiation and oxidative stress resistance mechanisms in *Deinococcus* species. *FEMS Microbiol. Rev.* **43**:19-52.

Makarova KS, Aravind L, Wolf YI, Tatusov RL, Minton KW, Koonin EV and Daly MJ. 2001. Genome of the extremely radiation-resistant bacterium *Deinococcus radiodurans* viewed from the perspective of comparative genomics. *Microbiol. Mol. Biol. Rev.* **65**:44-79.

McGrane R and Beattie GA. 2017. *Pseudomonas syringae* pv. syringae B728a regulates multiple stages of plant colonization via the bacteriophytochrome BphP1. *mBio* **8**:e01178-17.

Multamäki E, Nanekar R, Morozov D, Lievonen T, Golonka D, Wahlgren WY, Stucki-Buchli B, Rossi1 J, Hytönen VP, Westenhoff S, Ihalainen JA, Möglich A and Takala H. 2021. Comparative analysis of two paradigm bacteriophytochromes reveals opposite functionalities in two-component signaling. *Nat. Commun.* **12**:4394.

Nagano S. 2016. From photon to signal in phytochromes: similarities and differences between prokaryotic and plant phytochromes. *J. Plant. Res.* **129**:123-135.

Omelchenko MV, Wolf YI, Gaidamakova EK, Matrosova VY, Vasilenko A, Zhai M, Daly MJ, Koonin EV and Makarova KS. 2005. Comparative genomics of *Thermus thermophilus* and *Deinococcus radiodurans*: divergent routes of adaptation to thermophily and radiation resistance. *BMC Evol. Biol.* **5**:57.

Rottwinkel G, Oberpichler I and Lamparter T. 2010. Bathy phytochromes in rhizobial soil bacteria. *J. Bacteriol.* **192**: 5124-5133.

Saïd-Salim B, Mostowy S, Kristof AS and Behr MA. 2006. Mutations in *Mycobacterium tuberculosis* Rv0444c, the gene encoding anti-SigK, explain high level expression of MPB70 and MPB83 in *Mycobacterium bovis*. *Mol. Microbiol.* **62**:1251-1263.

Schmid AK and Lidstrom ME. 2002. Involvement of two putative alternative sigma factors in stress response of the radioresistant bacterium *Deinococcus radiodurans*. *J. Bacteriol.* **184**: 6182-6189.

Slade D and Radman M. 2011. Oxidative stress resistance in *Deinococcus radiodurans*. *Microbiol. Mol. Biol. Rev.* **75**:133-191.

Souza BM, Castro TL, Carvalho RD, Seyffert N, Silva A, Miyoshi A and Azevedo V. 2014. σ^{ECF} factors of gram-positive bacteria: a focus on *Bacillus subtilis* and the CMNR group. *Virulence* **5**:587-600.

Timmins J and Moe E. 2016. A decade of biochemical and structural studies of the DNA repair machinery of *Deinococcus radiodurans*: major findings, functional and mechanistic insight and challenges. *Comput. Struct. Biotechnol. J.* **14**:168-176.

Veyrier FJ, Nieves C, Lefrancois LH, Trigui H, Vincent AT and Behr MA. 2020. RskA is a dual function activator-inhibitor that controls SigK activity across distinct bacterial genera. *Front. Microbiol.* **11**:558166.

Vuillet L, Kojadinovic M, Zappa S, Jaubert M, Adriano JM, Fardoux J, Hannibal L, Pignol D, Verméglio A and Giraud E. 2007. Evolution of a bacteriophytochrome from light to redox sensor. *EMBO J.* **26**:3322-3331.

Wagner JR, Brunzelle JS, Forest KT and Vierstra RD. 2005. A light-sensing knot revealed by the structure of the chromophore-binding domain of phytochrome. *Nature* **438**:325-331.

White O, Eisen JA, Heidelberg JF, Hickey EK, Peterson JD, Dodson RJ, Haft DH, Gwinn ML, Nelson WC, Richardson DL, Moffat KS, Qin H, Jiang L, Pamphile W, Crosby M, Shen M, Vamathevan JJ, Lam P, McDonald L, Utterback T, Zalewski C, Makarova KS, Aravind L, Daly MJ, Minton KW, Fleischmann RD, Ketchum KA, Nelson KE, Salzberg

S, Smith HO, Venter JC and Fraser CM. 1999. Genome sequence of the radioresistant bacterium *Deinococcus radiodurans* R1. *Science* **286**:1571-1577.

Wu L, McGrane RS and Beattie GA. 2013. Light regulation of swarming motility in *Pseudomonas syringae* integrates signaling pathways mediated by a bacteriophytochrome and a LOV Protein. *mBio*. **3**:e00334-13.

Xue P, El Kurdi A, Kohler A, Ma H, Kaeser G, Ali A, Fischer R, Krauß N and Lamparter T. 2019. Evidence for weak interaction between phytochromes Agp1 and Agp2 from *Agrobacterium fabrum*. *FEBS Lett*. **593**:926-941.

Zhang C, Zhou Z, Zhang W, Chen Z, Song Y, Lu W, Lin M and Chen M. 2015. The site-directed A184S mutation in the HTH domain of the global regulator IrrE enhances *Deinococcus radiodurans* R1 tolerance to UV radiation and MMC shock. *J. Microbiol. Biotechnol*. **25**:2125-2134.

Received: 29 September 2021
Revised: 21 December 2021
Revision accepted: 21 December 2021